Anisotropic tomography for TTI and VTI media

Yang He and Jun Cai, TGS*

Summary

A simultaneous anisotropic tomographic inversion algorithm is developed. Check shot constraints and appropriate algorithm preconditioning play an important role in separating the trade-off between the velocity and Thomsen's anisotropic parameters. Field data examples show the feasibility for this technique.

Introduction

As the demand increases to improve the subsurface image accuracy, anisotropic imaging (both Tilted Transverse Isotropic (TTI) and Vertical Transverse Isotropic (VTI)) has gradually becomes routine processing. However, optimizing anisotropic model building technology and the work flow remains an active and challenging topic.

Tomography as a velocity model building tool has been studied and has become a routine processing tool (Zhou et al., 2001, Cai et al., 2006). Anisotropic tomography also has been studied as a way to build anisotropic models (Yuan et al., 2006 for 3D VTI; Zhou et al., 2004 for 2.5D TTI).

We developed a Focusing Analysis (FAN) approach for VTI and TTI anisotropic model building (Cai et al., 2009). The key for FAN is using check shot information to solve the trade-off between velocity and anisotropic parameters. In this study, we try to combine the strengths of FAN and tomography, to provide a robust solution for anisotropic model building.

Anisotropic tomography and synthetic example

A previous study (Audebert and Dirks, 2006) indicates that by assuming that the tilt medium coincides with the dip of the structure the decoupling of the anisotropic parameters is greatly simplified. In this study, we assume the tilt axis is perpendicular to the structure dip. For both TTI and VTI, the tilt axis is the input to the program; the same program can handle both TTI and VTI media. Velocity and the Thomsen parameters are the only unknowns that need to be inverted.

TTI tomography can be described by solving the linear system,

$$\begin{bmatrix} \frac{\partial t}{\partial v_o} & \frac{\partial t}{\partial \delta} & \frac{\partial t}{\partial \varepsilon} \end{bmatrix} \begin{bmatrix} \Delta v_0 \\ \Delta \delta \\ \Delta \varepsilon \end{bmatrix} = r$$

where v_0 is the velocity, δ and ε are Thomsen's parameters, and r is the vector of the traveltime residuals. To solve this linear system, a nonlinear preconditioned conjugate gradient algorithm is applied.

Accurate picking is a critical part of tomographic inversion. For anisotropic tomography, a simple parabolic or hyperbolic curve is not sufficient to distinguish the impact of the velocity and the anisotropy. We develop a two-parameter polynomial curve to pick the depth residuals. The curvature can be described as

$$C = C_2 x^2 + C_4 x^4$$

The major contribution to the second order term coefficient (C_2) should belong to the velocity; the main anisotropic contribution should be reflected in the fourth order term coefficient (C_4). Internally the two-parameter fitting is used to invert the velocity and Thomsen's parameters simultaneously.

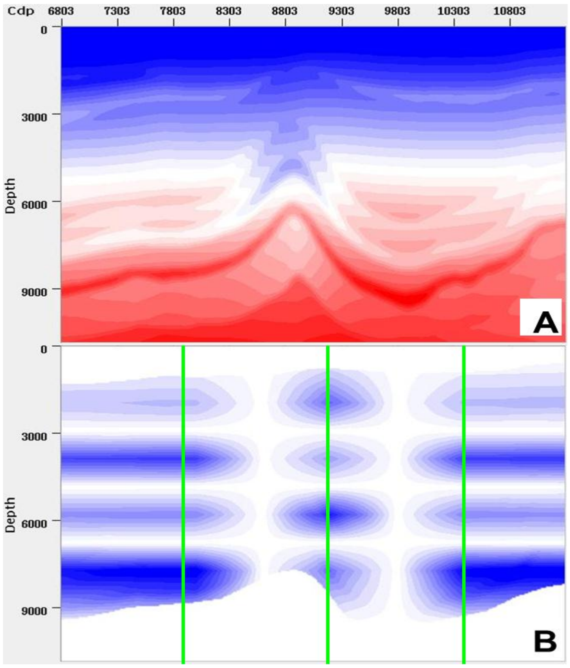

Figure 1: Original velocity model (A) (models courtesy BP) and velocity perturbation (B). Three check shots (green lines) are used.

To validate the algorithm, the BP 2008 TTI benchmark model was used. The velocity perturbation (Figure 1B) was added to the original velocity model (Figure 1A) to generate the initial velocity model.

After the initial isotropic migration, the polynomial picking was performed on the original Common Image Gathers (CIGs) (Figure 2A). The two-term polynomial picking of the moveout is able to flatten the CIGs around the complex area (Figure 2B).

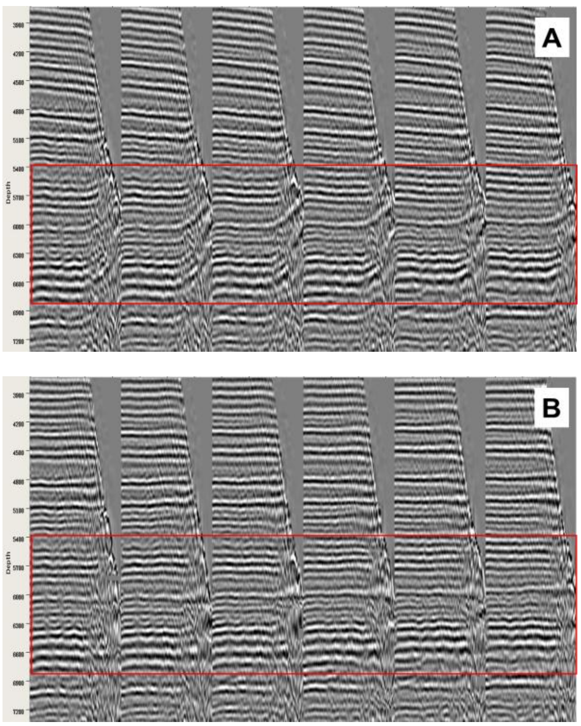

Figure 2: Depth residual picking and residual moveout (A) before residual moveout correction and (B) after residual moveout correction.

Two anisotropic tomography scenarios are tested (Figure 3). From the same initial isotropic model, three check shot constraints were used in one experiment (dark blue curves), but not in the other one (magenta curves). For the shallow part, because of the wide reflection angle coverage, there is better control over the velocity and anisotropic parameter contributions. For both scenarios, the inversion results provide reasonable answers compared to the true solution (light blue curves). But for the deep part, where there is a lack of reflection angle resolution (arrows); the inversion results at three checkshot locations indicate that the checkshots helped to resolve the trade-off issues and drive the velocity (Figure 3A) closer to the correct solution. Still the small velocity errors in the deep part could introduce large uncertainty for the anisotropic parameters. Because of this uncertainty, in practice, we normally dampen the anisotropic parameters gradually to a small constant.

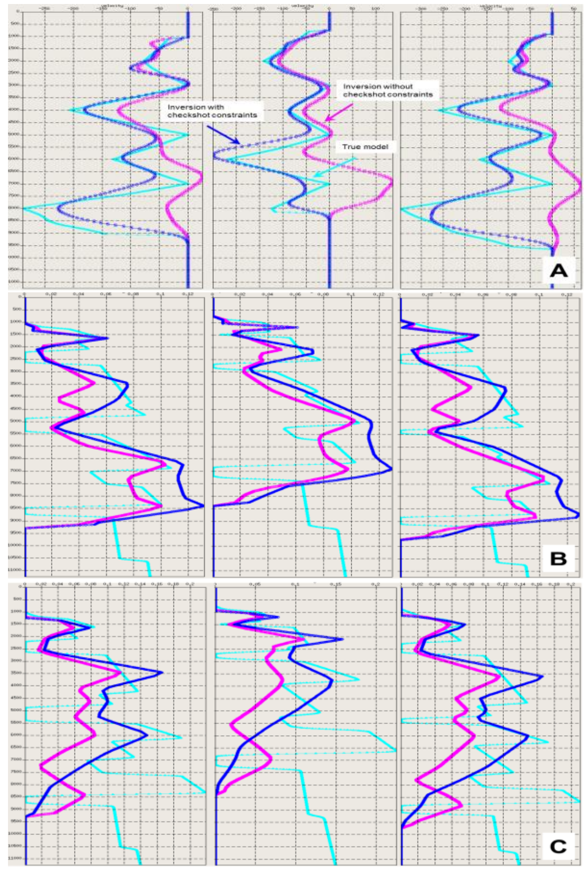

Figure 3: Anisotropic tomographic inversion results for velocity (A), delta (B) and epsilon (C) at three check shot locations. The light blue curves are the true model, and the magenta curves are the inversion results without check shot constraints, the dark blue curves are the inversion results with check shot constraints.

Figure 4 shows the corresponding CIGs for the isotropic migration (Figure 4A), for the TTI migration using models derived without (Figure 4B) and with (Figure 4C) check shot constraints, respectively. CIGs for the model derived with check shot constraints (Figure 4C) are only slightly flat compared with CIGs for the model derived without check shot constraints (Figure 4B). The main difference is the reflector depth difference (blue arrows). Consequently, for the deep portion, check shots play an important role, since data can provide only limited reflection angle information.

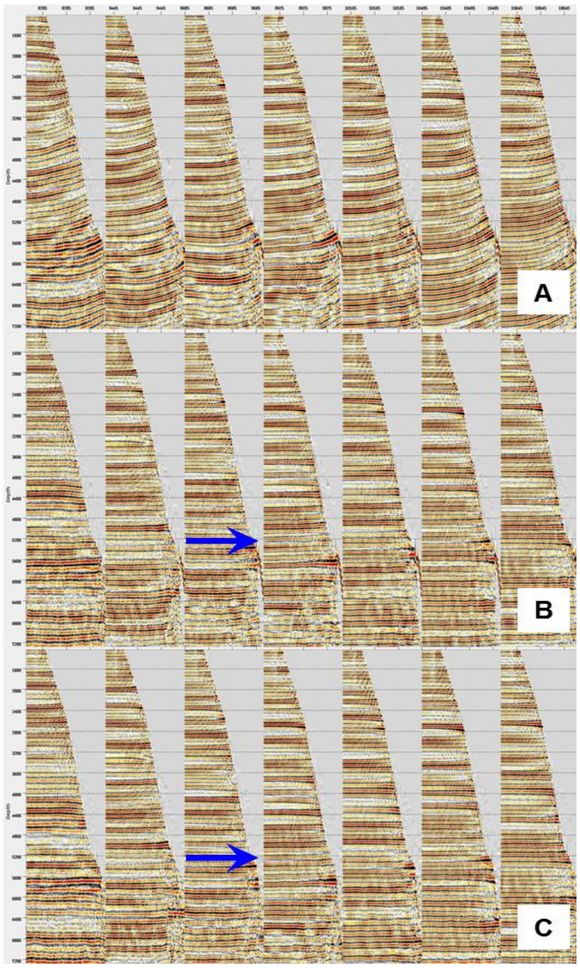

Figure 4: CIGs for initial isotropic migration (A); CIGs from anisotropic tomography without check shot constraints (B), and with check shot constraints (C).

Field data examples

TTI anisotropic tomography was tested on data from TGS' Kepler WAZ survey (Figure 5). The initial isotropic model was built from check shots; followed by an isotropic migration. Figure 6A shows the CIGs for the isotropic migration around a check shot location. Two approaches were used to update the anisotropic and velocity models.

- Two-pass model building approach: first, FAN is applied at each check shot location; followed by horizon-guided interpolation to build the smooth anisotropic model. Then isotropic tomography is applied to derive the v_o model. Figure 6B shows the CIGs from this two-pass approach.
- One-pass approach: simultaneous anisotropic tomography is used to derive velocity, epsilon and delta at the same time, while check shots are used as constraints.

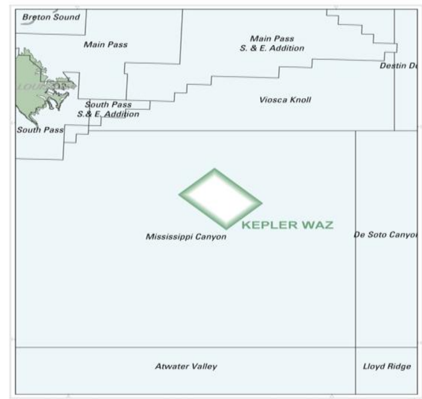

Figure 5: Map shows the Kepler WAZ survey.

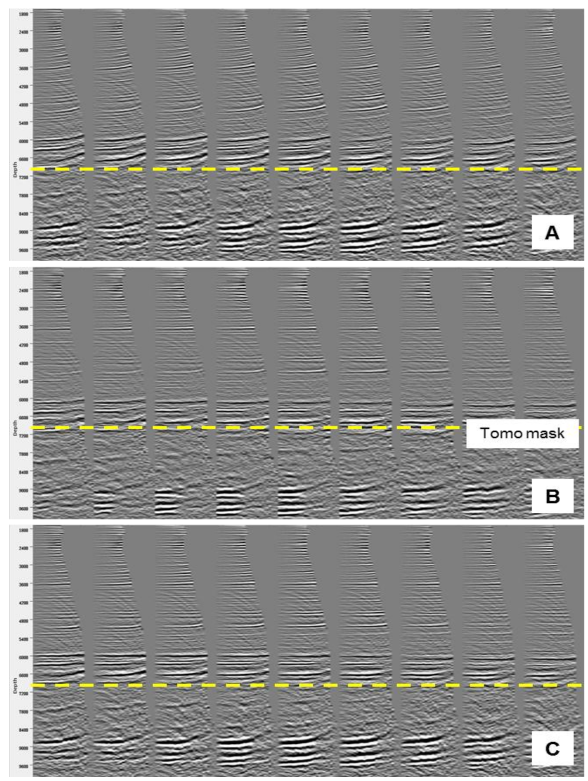

Figure 6: Field data CIGs. (A) Isotropic migration. (B) CIGs using two-pass model building solution. (C) CIGs for simultaneous tomography solution.

Comparing these two scenarios, some vertical shifts appear between the two migration results (Figure 6B and Figure 6C), which indicate that check shot recalibration is needed for the two-pass approach in next iteration.

The stack section comparison between the initial isotropic migration and the two model building approaches is shown in Figure 7. The improvement in the stacks for the two-pass and simultaneous anisotropic tomography methods can be attributed to flatter CIGs.

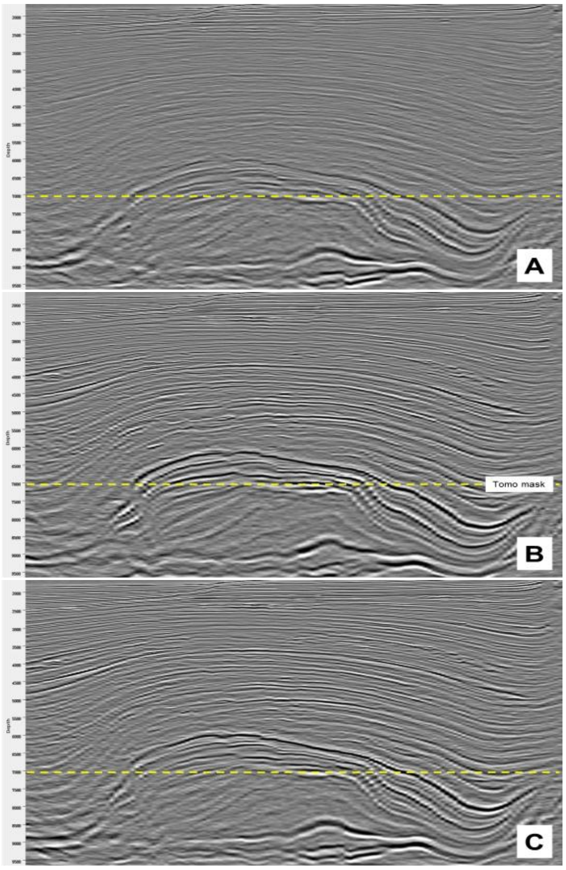

Figure 7: Stack for initial isotropic migration (A), one iteration two-pass model building (B), and simultaneous anisotropic tomography (C).

Figure 8 shows the velocity model derived from the two different approaches. We can see that with the simultaneous anisotropic tomography solution, the velocity model is somewhat simpler and smoother compared with the two-pass approach. Also, there is a velocity slowdown around the check shot location in the shallow portion, which is consistent with the observation from CIGs. The 3D delta model (Figure 8C) and epsilon model (Figure 8D) show a generally smoothly varying trend, which follows the structure.

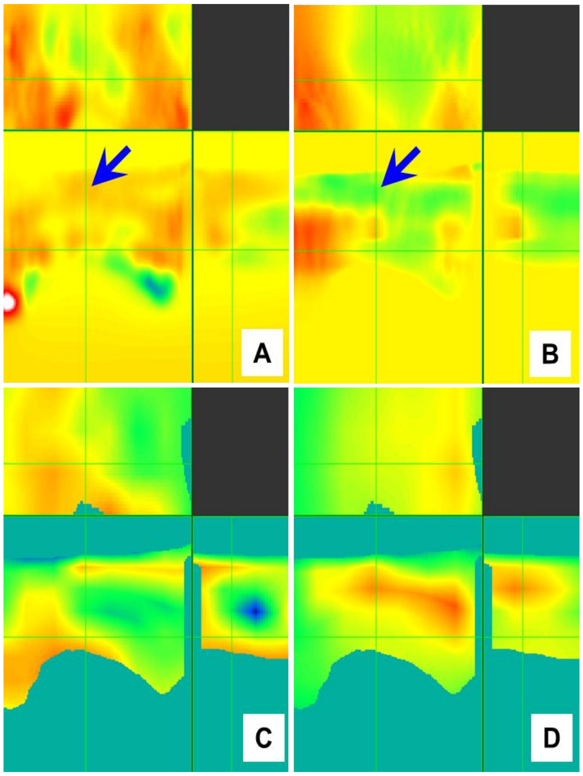

Figure 8: Velocity model comparison between the two-pass approach (A) and the simultaneous anisotropic tomography solution (B). (C) and (D) are corresponding 3D delta and epsilon models respectively.

Conclusions

The synthetic example results show that the simultaneous anisotropic tomography algorithm can resolve the trade-off between velocity and anisotropic parameters in the shallow part, where there is enough reflection angle coverage. In the deep portion, which lacks thorough reflection angle coverage, check shots will be needed to help improve the accuracy. The field data example shows that with the help of check shot constraints, simultaneous anisotropic tomography can improve model convergence.

Acknowledgement

Authors would like to thank Bin Wang and Zhiming Li for their helpful advice during this project, and Laurie Geiger, Simon Baldock and Chuck Mason for proof reading. We thank the management of TGS for permission to publish this paper.

EDITED REFERENCES

Note: This reference list is a copy-edited version of the reference list submitted by the author. Reference lists for the 2011 SEG Technical Program Expanded Abstracts have been copy edited so that references provided with the online metadata for each paper will achieve a high degree of linking to cited sources that appear on the Web.

REFERENCES

Audebert, F. and V. Dirks, 2006, TTI anisotropic depth migration: What tilt estimate should we use?: 76th Annual International Meeting, SEG, Expanded Abstracts, 2382–2386.

Cai, J., Y. He, Z. Li, B. Wang, and M. Guo, 2009, TTI/VTI anisotropy parameters estimation by focusing analysis, Part I: Theory: 79th Annual International Meeting, SEG, Expanded Abstracts, 301–305.

Cai, J., M. Witcombe, J. Weigant, and J. Du, 2006, Depth-velocity model building using multiscale tomography —Part 1: 76th Annual International Meeting, SEG, Expanded Abstracts, 3359–3363.

Yuan, J., X. Ma, S. Lin, D. Lowrey, 2006, P-wave tomographic velocity updating in 3D inhomogeneous VTI media: 76th Annual International Meeting, SEG, Expanded Abstracts, 3368–3372.

Zhou, D., S. Pham, S. Gray, and B. Wang, 2004, Tomographic velocity analysis in strong anisotropic TTI media: 74th Annual International Meeting, SEG, Expanded Abstracts, 2347–2350.